Numerical study of oblique detonation wave initiation in a stoichiometric hydrogen-air mixture

Tao Wang, Yining Zhang, Honghui Teng, Zonglin Jiang, and Hoi Dick Ng

Citation: Physics of Fluids **27**, 096101 (2015); doi: 10.1063/1.4930986
View online: http://dx.doi.org/10.1063/1.4930986
View Table of Contents: http://scitation.aip.org/content/aip/journal/pof2/27/9?ver=pdfcov
Published by the AIP Publishing

PHYSICS OF FLUIDS **27**, 096101 (2015)

Numerical study of oblique detonation wave initiation in a stoichiometric hydrogen-air mixture

Tao Wang,[1] Yining Zhang,[2] Honghui Teng,[1] Zonglin Jiang,[1] and Hoi Dick Ng[3]

[1]*State Key Laboratory of High Temperature Gas Dynamics, Institute of Mechanics, Chinese Academy of Sciences, Beijing 100190, China*

[2]*State Key Laboratory of Laser Propulsion and Application, Beijing Power Machinery Research Institute, Beijing 100074, China*

[3]*Department of Mechanical and Industrial Engineering, Concordia University, Montreal, Quebec H3G 1M8, Canada*

(Received 3 March 2015; accepted 27 August 2015; published online 17 September 2015)

Two-dimensional, oblique detonations induced by a wedge are simulated using the reactive Euler equations with a detailed chemical reaction model. The focus of this study is on the oblique shock-to-detonation transition in a stoichiometric hydrogen-air mixture. A combustible, gas mixture at low pressure and high temperature, corresponding to the realistic, inflow conditions applied in oblique detonation wave engines, is presented in this study. At practical flight conditions, the present numerical results illustrate that oblique detonation initiation is achieved through a smooth transition from a curved shock, which differs from the abrupt transition depicted in the previous studies. The formation mechanism of this smooth transition is discussed and a quantitative analysis is carried out by defining a characteristic length for the initiation process. The dependence of the initiation length on different parameters including the wedge angle, flight Mach number, and inflow Mach number is discussed. Despite the hypothetical nature of the simulation configuration, the present numerical study uses parameters we deem relevant to practical conditions and provides important observations for which future investigations can benefit from in reaching toward a rigorous theory of the formation and self-sustenance of oblique detonation waves. © *2015 AIP Publishing LLC.* [http://dx.doi.org/10.1063/1.4930986]

I. INTRODUCTION

In recent years, high efficiency propulsion systems have generated great interest for their use in the development of air-breathing hypersonic aircraft. The concept of oblique detonation waves has led to the development of Oblique Detonation Wave Engines (ODWEs)[1] and Ram Accelerators.[2] This class of propulsion systems not only shares advantages with the Scramjet (Supersonic combustion ramjet) but also achieves a high thermal cycle efficiency through the use of the detonation mode of combustion.[3] However, it remains technically challenging, for propulsion applications, to establish a steady oblique detonation in high-speed, combustible mixtures. A more fundamental understanding of the oblique detonation structure and instability is required to develop workable engines.

In early oblique detonation wave research, the problem was usually simplified into an oblique shock wave with a post-shock, energy release zone attached to the wedge.[4,5] With the use of shock polars, the coupling relation of the oblique shock and combustion is discussed and analyzed.[6–8] Nevertheless, studies demonstrate that the realistic structure near the wedge front tip is rather complex. Li *et al.*[9] numerically simulated the oblique detonation and observed a structure composed of a nonreactive oblique shock, an induction region, a set of deflagration waves, and the oblique detonation surface. This structure was verified experimentally[10] and is often considered the "standard structure" used widely in many subsequent studies. Based on this structure, Sislian *et al.*[11,12] studied near-Chapman–Jouguet (CJ), oblique detonation waves and the propulsive performance of oblique detonation engines. Papalexandris[13] and Choi *et al.*[14] observed a fine scale structure characterized by a

"saw tooth" flame on the oblique detonation surfaces. The formation of this fine structure is attributed to the instability of the coupling between the oblique shock and the chemical reaction. Although the formation of triple points would be suppressed by high degrees of overdrive, recent studies by Teng *et al.*[15,16] show that oblique detonation surfaces are unconditionally unstable, and their dynamics is similar to that of multi-dimensional cellular detonations. Small scale, instability features are observed on the oblique detonation surface, similar to the unstable frontal structure of a normal cellular detonation.[16–18] Moreover, oblique detonation waves induced by conical[19,20] and spherical projectiles[21,22] have been investigated in the literature. Similar fine scale structures were observed.

It is worth noting that the previous studies mainly focused on the instability of oblique detonation surfaces; however, the oblique shock-to-detonation transition has not yet attracted enough attention. Studies suggest that both abrupt and smooth transition structures exist.[23,24] The abrupt structure is achieved by a multi-wave point connecting the oblique shock and the detonation surface, while the smooth transition originates from a curved shock instead of the multi-wave point. Teng and Jiang[25] analyzed the structural differences of these two transition processes as a function of different chemical and aerodynamic parameters, and from there proposed criteria to characterize the transition type. Furthermore, the observed transient structures are also dependent on the inflow Mach number toward the wedge and chemical activation energy,[26,27] making the modeling of realistic oblique detonations even more complex.

The transition from oblique shock to detonation is at the origin of successful oblique detonation initiation. Consequently, its research is crucial in the design of ODWE. Recent studies[28–30] on normal detonation initiation have demonstrated that both aerodynamic and mixture thermodynamic properties greatly influence the initiation of detonation. However, a deep knowledge of the oblique structure found in ODWE is still lacking and must be fully addressed. For simplicity, most of the previous studies[5–9,13–20] used simplified chemical reaction models, mainly the one-step irreversible Arrhenius kinetic model. In addition, the inflow parameters are usually set artificially, deviating far from those in actual ODWE applications. To address the aforementioned issues, oblique detonation waves in a stoichiometric hydrogen-air mixture are investigated in this study with detailed chemistry. The inflow parameters are chosen to simulate the flow conditions in ODWE at high altitude. The numerical results will illustrate that the initiation of oblique detonation waves at these practical flow conditions is achieved by a smooth shock-to-detonation transition. The mechanism of ODW formation from the smooth transition is also studied, and the effect of the flight Mach number, inflow Mach number, and wedge angle is analyzed quantitatively by defining a characteristic length scale for the initiation process.

II. MATHEMATICAL MODEL AND COMPUTATIONAL DETAILS

A schematic of an ODWE[31] and the wedge-induced oblique detonation is shown in Fig. 1. M_o denotes the flight number of the aircraft and M_1 is the inflow Mach number of the combustible gas mixture inducing the oblique detonation wave from the wedge. One simplification used in this study is that the fuel mixing in supersonic flow is not considered. In other words, this study assumes the inflow to be well-mixed and focuses primarily on the resulting oblique detonation structure. Considering a flight altitude of 30 km and Mach number of 10, the flow is first pre-compressed twice by weak oblique shock waves in the inlet diffuser. The combustible inflow then reflects on the two-dimensional wedge and first generates an oblique shock wave. The shock wave may trigger exothermic chemical reactions and subsequently induce an oblique detonation wave downstream. For the present numerical study, the computational domain is bounded by the dashed zone shown in Fig. 1, whose coordinates are aligned with the wedge surface.

Previous results[23,32] demonstrated that the viscosity has negligible effects on the ODW structure. In keeping with previous simulations, an inviscid assumption is also invoked in this work, and as a result boundary layer effects are not included in this study. The governing equations are thus simplified to the two-dimensional multi-species Euler equations written as follows:

$$\frac{\partial \mathbf{U}}{\partial t} + \frac{\partial \mathbf{F}}{\partial x} + \frac{\partial \mathbf{G}}{\partial y} = \mathbf{S}, \tag{1}$$

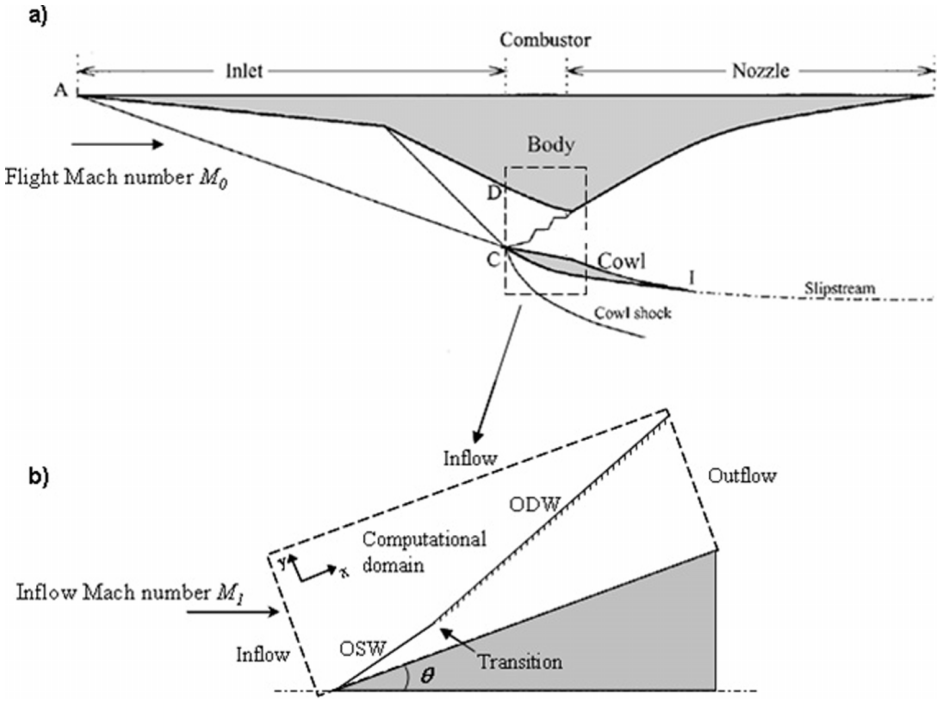

FIG. 1. Schematic of (a) an ODWE[31] and (b) the wedge-induced oblique detonation from a flowing combustible gas mixture.

where

$$\mathbf{U}=\begin{Bmatrix}\rho_1\\ \vdots\\ \rho_n\\ \rho u\\ \rho v\\ e\end{Bmatrix},\ \mathbf{F}=\begin{Bmatrix}\rho_1 u\\ \vdots\\ \rho_n u\\ \rho u^2+p\\ \rho uv\\ (e+p)\,u\end{Bmatrix},\ \mathbf{G}=\begin{Bmatrix}\rho_1 v\\ \vdots\\ \rho_n v\\ \rho uv\\ \rho v^2+p\\ (e+p)\,v\end{Bmatrix},\ \mathbf{S}=\begin{Bmatrix}\omega_1\\ \vdots\\ \omega_n\\ 0\\ 0\\ 0\end{Bmatrix}. \tag{2}$$

In the above equations, the total density and total energy are calculated by

$$\rho=\sum_{i=1}^{n}\rho_i,\ e=\rho h-p+\frac{1}{2}\rho\left(u^2+v^2\right), \tag{3}$$

where specific enthalpy can be written as $h=\sum_{i=1}^{n}\rho_i h_i/\rho$ with h_i obtained from thermodynamic data of each individual species. The equation of state is

$$p=\sum_{i=1}^{n}\rho_i\frac{R_0}{w_i}T, \tag{4}$$

where w_i is the molecular weight and T is the gas temperature; ω_i is the species specific mass production rate, which is dictated by the chemical reaction model. The governing equations are then solved on an adaptive, unstructured, quadrilateral mesh[33] using the MUSCL-Hancock scheme.[34] This numerical scheme approaches second-order accuracy in space and time by constructing the Riemann problem on the inter-cell boundary through the following equations:

$$\begin{aligned}\bar{U}_i^L&=U_i^L+\frac{\Delta t}{2\Delta x}\left[F\left(U_i^L\right)-F\left(U_i^R\right)\right],\\ \bar{U}_i^R&=U_i^R+\frac{\Delta t}{2\Delta x}\left[F\left(U_i^L\right)-F\left(U_i^R\right)\right].\end{aligned} \tag{5}$$

The solution of the associated Riemann problem is computed by the HLLC approximate Riemann solver. A hydrogen/air chemical reaction model[35] is selected from the widely used CHEMKIN package and the mechanism consists of 11 species (H_2, O_2, O, H, OH, HO_2, H_2O_2, H_2O, N_2, N, and NO) and 23 elementary reactions. The CHEMKIN database of thermodynamic parameters was used without modification. The stiff nature of the problem due to the chemical reaction calculation is solved by the DVODE package.[36] A stoichiometric hydrogen-air mixture with H_2:O_2:N_2 = 2:1:3.76 is used. The slip reflecting boundary condition is used on the wedge surface and the other boundaries are interpolated under the assumption of zero first-order derivatives of all flow parameters. Unless specified otherwise, a computational domain of 60 mm × 20 mm is used and initially covered by a primary mesh of 0.2 mm × 0.2 mm. Adaptive mesh refinement (AMR) is based on the density gradient,[33] and the highest numerical resolution contains the finest grid size of 0.025 mm with three levels of refinement. The wedge begins at $x = 1.0$ and the length scale is in mm for all figures shown in Secs. III and IV.

III. NUMERICAL RESULTS AND DISCUSSION

To simulate the flow dynamics in an ODWE, the flight conditions need to be prescribed to determine the inflow pressure and temperature. Air-breathing aircraft equipped with an ODWE is typically designed to operate at high altitude (about 25-35 km) and can cover a range of Mach numbers. Considering a flight altitude of 30 km and a flight Mach number M_o of 10, the ambient flow is pre-compressed twice by weak oblique shock waves in the aircraft inlet. The implicit relation between the oblique shock angle β and deflection angle ϕ is given by

$$\tan^3\beta + A\tan^2\beta + B\tan\beta + C = 0, \tag{6}$$

where

$$\begin{aligned} A &= \frac{1 - M^2}{\tan\phi\left[1 + (\gamma - 1)M^2/2\right]}, \\ B &= \frac{1 + (\gamma + 1)M^2/2}{1 + (\gamma - 1)M^2/2}, \\ C &= \frac{1}{\tan\phi\left[1 + (\gamma - 1)M^2/2\right]}. \end{aligned} \tag{7}$$

Using the above equations, the oblique shock angle β can be calculated. The latter can then be used to determine the inflow pressure and temperature. Considering a typical deflection angle $\phi = 12.5°$ and a resulting inflow Mach number $M_1 = 4.3$, a static pressure of approximately 56 kPa and a static temperature of 1021 K are obtained. In this study, the wedge angle θ inducing the oblique detonation is varied between 11° and 20°. The flight Mach number M_o and altitude have complex effects on pre-detonation inflow parameters. The flow is first simplified in this computational study such that the inflow Mach number M_1 varies between 4.0 and 5.0 without considering the change in static pressure and temperature. Afterward, the effects of inflow pressure and temperature, associated with the variation of flight Mach number M_o, are simulated and discussed.

A. Structures of oblique detonation waves

The oblique detonation structure resulting from an inflow Mach number M_1 of 4.3 and wedge angle of 15° is shown in Fig. 2. Notably, it can be observed that this structure is different from the abrupt transition considered in most of the previous studies. The transition is smooth with a curved shock and there is no obvious contact surface in the combustion products. In order to verify the effect of numerical grid resolution on such observations, detonation simulations with different grid sizes are carried out using the same initial and mixture conditions. Figure 3 compares the pressure field with different grid sizes. The upper portion shows simulation results with the finest grid of 0.0125 mm and the lower portion shows the results with the grid of 0.025-mm pitch. It can be observed that the difference is negligible. A resolution of 0.025 mm is therefore considered sufficient to study this problem and is selected as the finest grid size. Furthermore, using the grid size of 0.025 mm yields

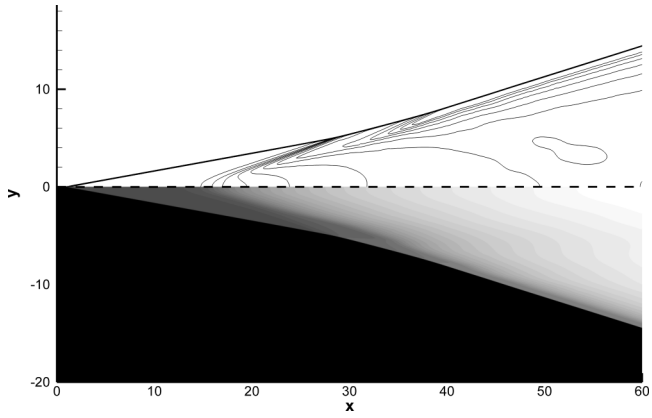

FIG. 2. Pressure (upper) and temperature (lower) fields in the case of an inflow Mach number M_1 of 4.3 and wedge angle of 15°.

about 10 grid points per half-reaction zone length along the streamline behind the corresponding overdriven detonation. The same effective grid resolution was also used in recent studies,[15,16] which demonstrates that both the structure and instability of oblique detonation surfaces can be correctly captured with this resolution. The oblique detonation structure given in both Figs. 2 and 3 depicts a smooth transition, which is different from the widely studied abrupt transition. It is worth noting again that oblique shock and detonation surfaces are connected by a multi-wave turning point in the abrupt transition, while surfaces in the smooth transition are connected by a curved shock.

Figure 4 shows pressure and temperature along different lines parallel to the x-axis, i.e., the wedge surface, demonstrating different combustion characteristics in this structure. Along the line $y = 3$, a long induction zone can be seen with about 10 mm of separation between the shock and the pressure peak induced by the heat release. Along the line $y = 6$, the oblique shock is stronger, increasing the pressure and temperature to a higher level than along the line $y = 3$. This results in a shorter induction zone, and the heat release is intensified. The line $y = 9$ corresponds to the oblique detonation surface, demonstrating the fully coupled structure between the oblique shock and the chemical reaction. The pressure and temperature along the line $y = 6$ are different from those of a fully established oblique detonation. This region can be viewed as an intermediate structure during the smooth transition of the oblique shock to oblique detonation.

To analyze the coupling between the oblique shock and subsequent heat release, Fig. 5 shows the induction zone length in the case of an inflow Mach number M_1 of 4.3 and wedge angle of 15°. Given the same combustible mixture with the same detailed chemical reaction mechanism, the steady Zel'dovich-von Neumann-Döring (ZND) structure of the corresponding CJ detonation can be

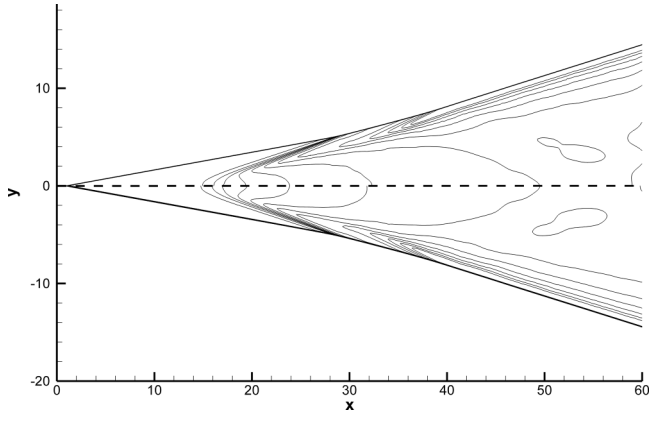

FIG. 3. Resolution study of the oblique detonation structure in the case of an inflow Mach number M_1 of 4.3 and wedge angle of 15°.

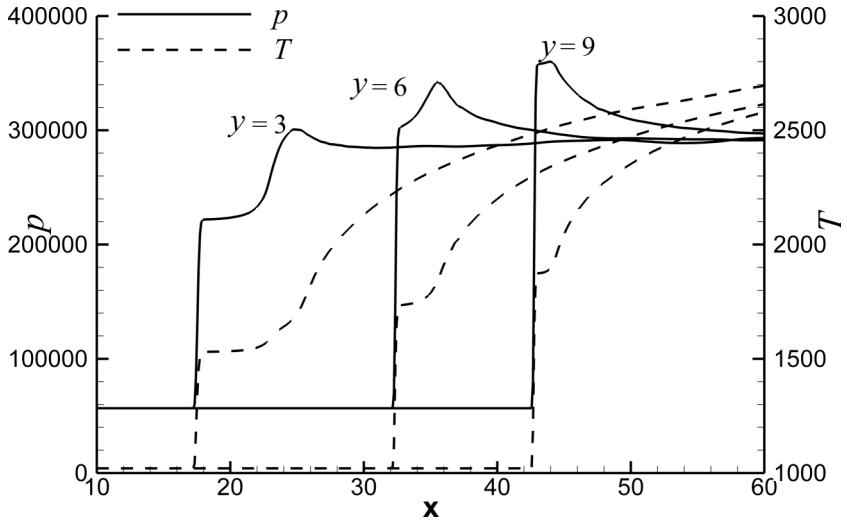

FIG. 4. Pressure and temperature along the line paralleled with the x-axis in the case of an inflow Mach number M_1 of 4.3 and wedge angle of 15°.

computed with the CHEMKIN package.[35] The latter indicates that the temperature at the end of the ZND induction zone is about 2070 K. This critical temperature is chosen here to identify the end of the induction zone in this study. The positions of the oblique shock and the end of the induction zone, along the line parallel with the y-axis, are shown through the right ordinate in Fig. 5. The induction zone length is deduced and shown through left ordinate in Fig. 5, representing the projection of real reaction zone length on the vertical direction. Using this approach, the disturbance of reaction zone can be magnified considerably.

It can be seen that the induction zone length increases first since there is no chemical heat release until about $x = 20$. The chemical reactions begin and subsequently induce the deflagration, resulting in a decrease of the induction zone. The length appears to decrease rapidly at first, but soon a plateau is established between $x = 30$ and $x = 35$. This plateau corresponds to the intermediate structure of the smooth transition, which is quasi-steady. The induction zone length decreases further and reaches its final stage gradually at about $x = 45$. It is worth noting that this length variation is quite different from that of the abrupt transition observed in the previous study.[15] In those cases, the induction zone length decreases drastically without the plateau to a minimum value near the multi-wave point. Then, a re-increasing trend can be observed so the length will reach the final value. However, there appears a quasi-steady plateau in this smooth transition, demonstrating the weak coupling of shock and heat

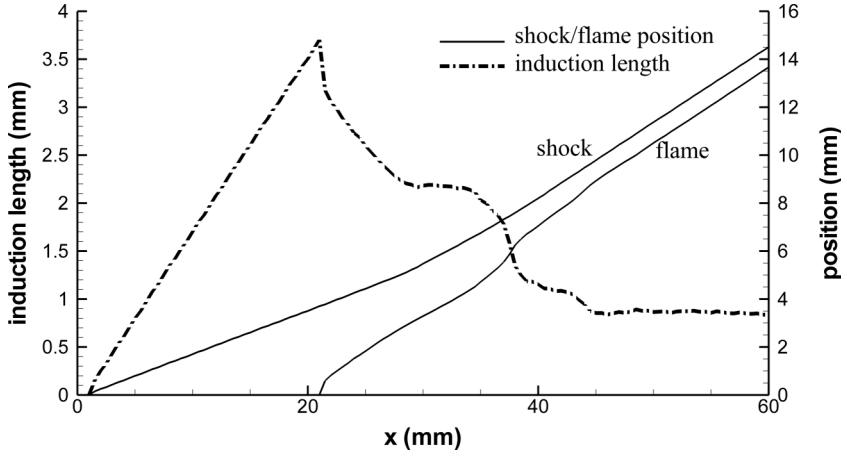

FIG. 5. Induction zone length in the case of an inflow Mach number M_1 of 4.3 and wedge angle of 15°.

release during this process. Similarly, this resembles the quasi-detonation in rough tubes,[37] and this plateau can perhaps be viewed as the quasi-steady structure in oblique detonation phenomena.

These aforementioned results are consistent with the previous study on the formation mechanism of different ODW structures.[25] The oblique detonation angle is greater than the oblique shock angle due to the heat release. A previous study[25] suggests that the abrupt transition appears if the angle difference is large, while the smooth transition appears if the angle difference is small. The critical value found in Ref. 25 is approximately 16°. The oblique detonation angle β_{det} can be calculated by

$$\frac{\tan\beta_{\mathrm{det}}}{\tan\left(\beta_{\mathrm{det}}-\theta\right)}=\frac{\left(\gamma+1\right)M^2\sin^2\beta_{\mathrm{det}}}{\gamma M^2\sin^2\beta_{\mathrm{det}}+1-\sqrt{\left(M^2\sin^2\beta_{\mathrm{det}}-1\right)^2-2\left(\gamma^2-1\right)M^2\sin^2\beta_{\mathrm{det}}Q}}. \tag{8}$$

If the heat release $Q = 0$, the oblique detonation angle becomes the oblique shock angle. In this study, the combustible gas mixture calculated from the ODWE flight conditions has a high temperature and a low pressure. Hence, the density of the inflow mixture is rather low, and the heat release is limited. This implies that the difference of oblique shock and detonation angle is small, leading toward the smooth transition in ODWE. Indeed, the angle difference for all cases in the present study lies between 5° and 10°.

B. Effects of wedge angle and inflow Mach number M_1

Oblique detonation structures in ODWE are influenced by several factors. In this study, the effect of two key parameters, namely, the wedge angle inducing the ODW and the inflow Mach number M_1, is further investigated. To study the effects of wedge angles, two more cases with $\theta = 13°$ and 17° are simulated and results are shown in Fig. 6. Notably, the initiation position moves downstream when the wedge angle decreases, and vice versa. For instance, for increasing wedge angles of 13°, 15°, and 17°, the corresponding initiation positions are approximately $x = 45$, 30, and 20 mm, respectively. Structures in the cases of different inflow Mach numbers are shown in Fig. 7, with the same wedge angle of 15°. It is found that the initiation position of both cases is located closely to $x = 30$ mm. Although a difference can be observed, the variation of the initiation position is not as significant as the change caused by the wedge angle.

Generally, numerical results show that the initiation position is insensitive to the inflow Mach number M_1, but sensitive to the wedge angle θ. The initiation process is rather complex and significantly influenced by post-shock thermodynamic parameters and wave dynamics.[27] However, one can notice that in these cases, the inflow gas mixtures have indeed reached a sufficiently high temperature close to the auto-ignition limit before interacting with the wedge, so initiation can be viewed as a shock-accelerating ignition. In this case, the initiation is strongly dependent on temperature and sensitive to the oblique shock strength. A wedge angle of 15° produces a post-oblique-shock temperature

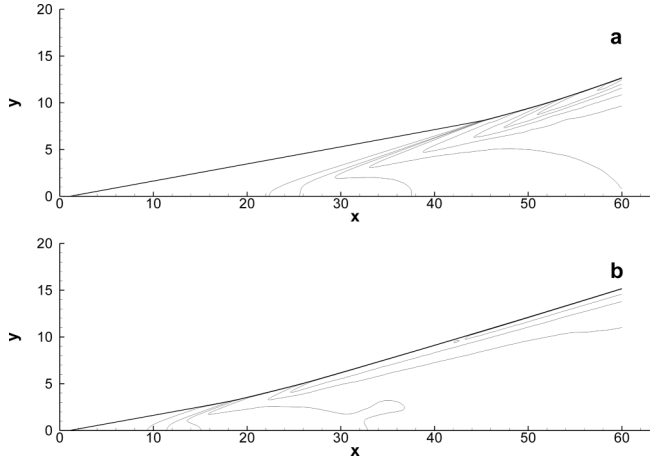

FIG. 6. Pressure field in the cases of an inflow Mach number M_1 of 4.3 and wedge angle of 13° (a) and 17° (b).

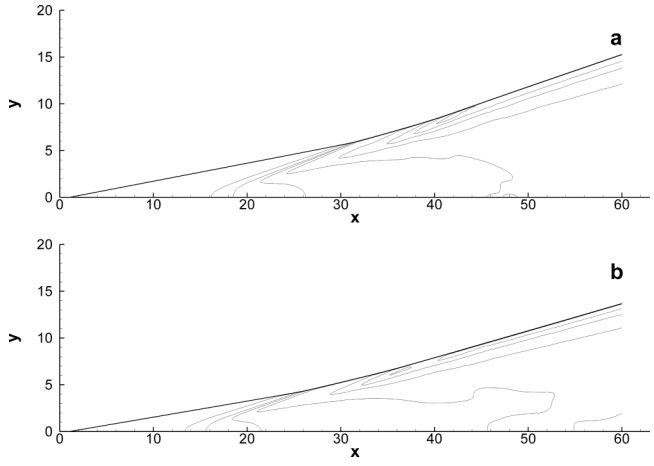

FIG. 7. Pressure field in the cases of a wedge angle 15°, and inflow Mach number M_1 of 4.1 (a) and 4.5 (b).

of approximately 1510 K and 1577 K for inflow Mach numbers $M_1 = 4.1$ and 4.5. On the other hand, with an inflow Mach number of 4.3, post-oblique-shock temperature is 1455 K and 1640 K in the cases of wedge angle 13° and 17°, respectively. Consequently, the wedge angle has a larger influence on the initiation position.

In order to further enhance the quantitative analysis, it is useful to define a characteristic length scale for the initiation process. We define an initiation length along the flow stream direction, parallel with the x-axis. It starts from the oblique shock and terminates at the end of induction zone, i.e., the point corresponding to the temperature value of 2070 K. Note that the lengths are different depending on the distance from the wedge, and thus, for convenience, the characteristic length of initiation is given by the maximum value for each case of (M_1, θ), always located on the wedge surface.

Figure 8 shows the characteristic length as a function of the wedge angle and inflow Mach number M_1. When $M_1 = 4.3$, the length decreases when the wedge angle increases as shown in Fig. 8(a). A similar relation between the characteristic length and M_1 can be observed in Fig. 8(b), with a wedge angle of 15°. However, it can be observed that the length dependence on the wedge angle and inflow Mach number M_1 is quite different. The length varies nonlinearly with the wedge angle, while the variation between the length and M_1 is almost linear. This suggests that M_1 itself can only vary in a narrow range, compared with the wedge angle. However, varying M_1 is different from wedge angle

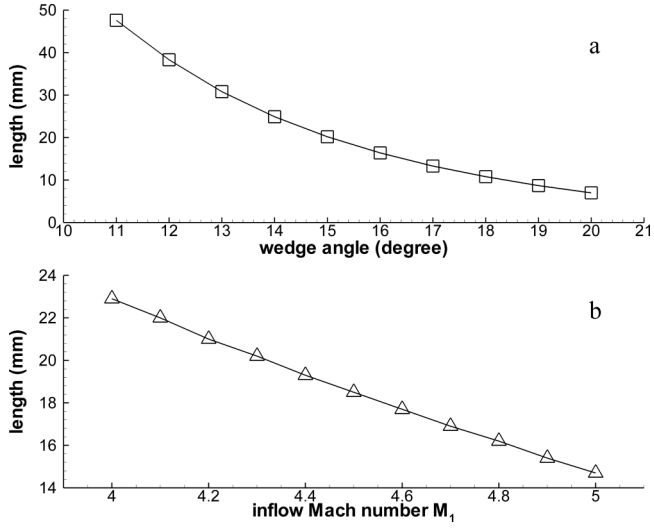

FIG. 8. Characteristic length as a function of the wedge angle with an inflow Mach number M_1 of 4.3 (a), and as a function of the inflow Mach number M_1 with a wedge angle of 15° (b).

TABLE I. Comparison of numerical and theoretical initiation length.

Angle	Numerical	Theoretical	Error (%)
11	47.6	38.40	21.0
12	38.3	30.85	21.5
13	30.8	24.94	21.6
14	24.9	20.02	22.7
15	20.2	16.28	23.2
16	16.4	13.18	24.2
17	13.3	10.72	25.1
18	10.8	8.68	26.5
19	8.7	7.04	27.5
20	7.0	5.69	28.8

because the former is limited by the flight conditions, while the latter can be chosen freely as an adjusting parameter to establish the oblique detonation. Larger intervals of wedge angle produce longer ranges of characteristic length, revealing the nonlinear dependence as shown in Fig. 8(b).

From the pressure field (e.g., Fig. 2), the coupling between pressure waves and combustion is apparent in close proximity below the oblique shock. Near the wedge, the mixture is completely burned, and pressure buildup and the formation of pressure waves are weak. According to this observation, the characteristic initiation length can be approximated theoretically based on post-oblique-shock conditions, which are available from classic aerodynamic theory. This theoretical result is based on the constant volume combustion calculation using the CHEMKIN package.[35] First, the post-oblique-shock species densities and temperature are used to simulate the constant volume combustion and to obtain the reaction time required to attain a mixture temperature of 2070 K. The theoretical initiation length is then calculated by multiplying the time with the post-oblique-shock velocity. Despite its simple formulation, this theoretical analysis provides a predictive approach for the general structure of oblique detonations. Table I shows the comparison of numerical and theoretical initiation length, together with the percentage difference between the two results. The theoretical length is smaller than the corresponding numerical one. In the cases listed in Table I, error increases monotonously, from 21.0% to 28.8%, with increasing wedge angle. Differences between the numerical and theoretical results are mainly from the constant volume assumption in the theoretical analysis. Also, in the case of high angles, the error becomes large due to the stronger gasdynamic effect. Despite the magnitude of the error, it is a good step for a more quantitative study on oblique detonations. It is important to note that the previous studies[27,38] on the initiation region have shown a rather complicated process, sometimes unpredictable, whose length depends on the balance of several factors. Although the method suggested in this study for the length prediction remains qualitative, it provides a simple first-step analysis, an improvement over a totally unpredictable phenomenon.

C. Effects of flight Mach number M_o

In order to study the effect of flight Mach number M_o, two more cases are simulated. The flight altitude remains 30 km, but the flight Mach number M_o is changed to 8 and 9. Also, the ambient flow is again compressed twice by weak oblique shock waves, with a deflection angle of 12.5°. Table II

TABLE II. Static pressure, temperature, and inflow Mach number M_1 in the cases of different flight Mach numbers M_o.

Flight Mach number M_o	P (kPa)	T (K)	Inflow Mach number M_1
10	56.0	1020.6	4.3
9	44.4	891.9	4.1
8	34.3	775.6	3.9

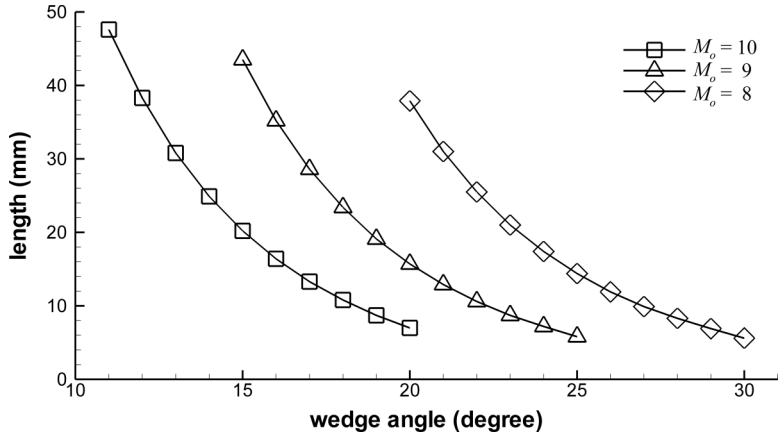

FIG. 9. Characteristic length as a function of the wedge angle with flight Mach numbers M_o of 10, 9, and 8.

shows the corresponding static pressure, temperature, and inflow Mach number M_1 for each of these additional cases.

The numerical results obtained with these parameters for different flight Mach numbers M_o are shown in Fig. 9. Although the length dependence on wedge angle is similar in the cases of different M_o, it is necessary to adjust the wedge angle to keep the characteristic length on the scale of several millimeters, which may be an important constraint in the ODWE design. For instance, to obtain an initiation length comparable to a wedge angle of 15° at a flight Mach number $M_o = 10$, the wedge angle should be increased to 18.5° and 23° in the cases of $M_o = 9$ and 8, respectively. Theoretical initiation lengths are also computed for these cases. In the case of $M_o = 9$, the error varies from 22.1% to 30.8% when the angle is changed from 15° to 25°. In the case of a flight Mach number $M_o = 8$, the error varies from 21.5% to 29.9% when the angle is changed from 20° to 30°. Considering the simple model and assumptions used for this prediction, as previously discussed, these errors are acceptable.

IV. CONCLUSION

In this study, oblique detonation waves in a stoichiometric hydrogen-air mixture are simulated with detailed chemistry. The focus of this paper is the initiation process of oblique detonation waves in practical conditions. In order to mimic the flow in an ODWE, the conditions of the combustible gas mixture with low pressure and high temperature are calculated from practical flight conditions. Under these conditions, numerical results show that the initiation is achieved through a transition from a smoothly curved shock to a detonation, not through the abrupt transition mechanism observed in the previous work. The formation mechanism of the present smooth transition is discussed and the result is found to be consistent with the previous theory in the literature. Based on the characteristic length of the initiation process, a quantitative analysis is performed. Results show the initiation length dependence on the wedge angle and the inflow Mach number M_1 is different. Furthermore, it is necessary to increase the wedge angle to keep the characteristic initiation length in a proper range when the flight Mach number is decreased.

Aside from their practical aspects, the results of this numerical investigation identify conditions at which initiation of the oblique detonation wave is through a transition from a smoothly curved shock to a detonation, a mechanism different from that generally considered in the previous work. The findings from the parametric study are of fundamental importance and useful for the development of further models of the formation and self-sustenance of oblique detonation waves.

ACKNOWLEDGMENTS

The research is supported by NSFC Nos. 11372333 and 51376165.

[1] K. Kailasanath, "Recent developments in the research on pulse detonation engines," AIAA J. **41**, 145–159 (2003).
[2] A. J. Higgins, "Ram accelerators: Outstanding issues and new directions," J. Propul. Power **22**, 1170–1187 (2006).
[3] P. Wokanski, "Detonative propulsion," Proc. Combust. Inst. **34**(1), 125–158 (2013).
[4] D. T. Pratt, J. W. Humphrey, and D. E. Glenn, "Morphology of standing oblique detonation waves," J. Propul. Power **7**(5), 837–845 (1991).
[5] M. J. Grismer and J. M. Powers, "Numerical predictions of oblique detonation stability boundaries," Shock Waves **6**, 147–156 (1996).
[6] J. M. Powers and K. A. Gonthier, "Reaction zone structure for strong, weak overdriven, and weak underdriven oblique detonations," Phys. Fluids A **4**(8), 2082–2089 (1992).
[7] J. M. Powers and D. S. Stewart, "Approximate solutions for oblique detonations in the hypersonic limit," AIAA J. **30**(3), 726–736 (1992).
[8] C. I. Morris, M. R. Kamel, and R. K. Hanson, "Shock-induced combustion in high-speed wedge flows," Proc. Combust. Inst. **27**, 2157–2164 (1998).
[9] C. Li, K. Kailasanath, and E. S. Oran, "Detonation structures behind oblique shocks," Phys. Fluids **4**, 1600–1611 (1994).
[10] C. Viguier, L. Figueira da Silva, D. Desbordes, and B. Deshaies, "Onset of oblique detonation waves: Comparison between experimental and numerical results for hydrogen-air mixtures," Proc. Combust. Inst. **26**, 3023–3031 (1996).
[11] J. P. Sislian, H. Schirmer, R. Dudebout *et al.*, "Propulsive performance of hypersonic oblique detonation wave and shock-induced combustion ramjets," J. Propul. Power **17**(3), 599–604 (2001).
[12] G. Fusina, J. P. Sislian, and B. Parent, "Formation and stability of near Chapman-Jouguet oblique detonation waves," AIAA J. **43**(7), 1591–1604 (2005).
[13] M. V. Papalexandris, "A numerical study of wedge-induced detonations," Combust. Flame **120**, 526–538 (2000).
[14] J. Y. Choi, D. W. Kim, I. S. Jeung *et al.*, "Cell-like structure of unstable oblique detonation wave from high-resolution numerical simulation," Proc. Combust. Inst. **31**, 2473–2480 (2007).
[15] H. H. Teng, Z. L. Jiang, and H. D. Ng, "Numerical study on unstable surfaces of oblique detonations," J. Fluid Mech. **744**, 111–128 (2014).
[16] H. H. Teng, H. D. Ng, K. Li *et al.*, "Cellular structure evolution on oblique detonation surfaces," Combust. Flame **162**, 470–477 (2015).
[17] M. Y. Gui, B. C. Fan, and G. Dong, "Periodic oscillation and fine structure of wedge-induced oblique detonation waves," Acta Mech. Sin. **27**, 922–928 (2011).
[18] J. Verreault, A. J. Higgins, and R. A. Stowe, "Formation transverse waves oblique detonations," Proc. Combust. Inst. **34**, 1913–1920 (2013).
[19] P. G. Harris, R. Farinaccio, R. A. Stowe *et al.*, "Structure of conical oblique detonation waves," AIAA Paper 2008-4687, 2008.
[20] J. Verreault, A. J. Higgins, and R. A. Stowe, "Formation and structure of steady oblique and conical detonation waves," AIAA J. **50**(8), 1766–1772 (2012).
[21] S. Maeda, S. Sumiya, J. Kasahara *et al.*, "Initiation and sustaining mechanisms of stabilized oblique detonation waves around projectiles," Proc. Combust. Inst. **34**(2), 1973–1980 (2013).
[22] S. Maeda, J. Kasahara, and A. Matsuo, "Oblique detonation wave stability around a spherical projectile by a high time resolution optical observation," Combust. Flame **159**, 887–896 (2012).
[23] L. Figueira da Silva and B. Deshaies, "Stabilization of an oblique detonation wave by a wedge: A parametric numerical study," Combust. Flame **121**, 152–166 (2000).
[24] A. F. Wang, W. Zhao, and Z. L. Jiang, "The criterion of the existence or inexistence of transverse shock wave at wedge supported oblique detonation wave," Acta Mech. Sin. **27**, 611–619 (2011).
[25] H. H. Teng and Z. L. Jiang, "On the transition pattern of the oblique detonation structure," J. Fluid Mech. **713**, 659–669 (2012).
[26] J. Y. Choi, E. J. R. Shin, and I. S. Jeung, "Unstable combustion induced by oblique shock waves at the non-attaching condition of the oblique detonation wave," Proc. Combust. Inst. **32**, 2387–2396 (2009).
[27] H. H. Teng, Y. Zhang, and Z. Jiang, "Numerical investigation on the induction zone structure of the oblique detonation waves," Comput. Fluids **95**, 127–131 (2014).
[28] B. Zhang, V. Kamenskihs, and H. D. Ng, "Direct blast initiation of spherical gaseous detonations in highly argon diluted mixtures," Proc. Combust. Inst. **33**(2), 2265–2271 (2011).
[29] B. Zhang, H. D. Ng, and J. H. S. Lee, "The critical tube diameter and critical energy for direct initiation of detonation in $C_2H_2/N_2O/Ar$ mixtures," Combust. Flame **159**(9), 2944–2953 (2012).
[30] B. Zhang, N. Mehrjoo, H. D. Ng *et al.*, "On the dynamic detonation parameters in acetylene-oxygen mixtures with varying amount of argon dilution," Combust. Flame **161**(5), 1390–1397 (2014).
[31] R. Dudebout, J. P. Sislian, and R. Oppitz, "Numerical simulation of hypersonic shock-induced combustion ramjets," J. Propul. Power **14**(6), 869–879 (1998).
[32] C. Li, K. Kailasanath, and E. S. Oran, "Effects of boundary layers on oblique detonation structures," AIAA Paper No. 93-0450, 1993.
[33] M. Sun and K. Takayama, "Conservative smoothing on an adaptive quadrilateral grid," J. Comput. Phys. **150**, 143–180 (1999).
[34] E. F. Toro, *Riemann Solvers and Numerical Methods for Fluid Dynamics*, 2nd ed. (Springer, Berlin, 1999).
[35] R. J. Kee, F. M. Rupley, E. Meeks *et al.*, "Chemkin-II: A Fortran chemical kinetics package for the analysis of gas-phase chemical and plasma kinetics," UC-405, SAND96–8216, Sandia National Laboratories, 1996.
[36] P. N. Brown, G. D. Byrne, and A. C. Hindmarsh, "VODE: A variable-coefficient ODE solver," SIAM J. Sci. Stat. Comput. **10**, 1038–1051 (1989).
[37] J. H. S. Lee, *The Detonation Phenomenon* (Cambridge University Press, New York, 2008).
[38] Y. Liu, D. Wu, S. Yao, and J. Wang, "Analytical and numerical investigations of wedge-induced oblique detonation waves at low inflow Mach number," Combust. Sci. Technol. **187**, 843–856 (2015).